UNIVERSITY OF CRETE

FACULTY OF SCIENCES AND ENGINEERING

DEPARTMENT OF PHYSICS

BACHELOR THESIS

Angular Sensitivity in a PT Symmetric Optical Lattice

Candidate:

STYLIANOS MILIOTIS

Matriculation number:

4135

Supervisor:

Prof. KOSTANTINOS MAKRIS

Supervisor:

Prof. GIORGIOS TSIRONIS

Heraklion

Academic year 2016/17

Acknowledgements

First and foremost, I would like to thank my thesis supervisors, Mr. Kostantinos Makris and Mr. Giorgios Tsironis. Especially, Mr. Kostantinos Makris for his support, assistance over the last year and dedicated involvement as well, in every step throughout the process of writing this thesis and beyond, for helping me get my studies to the next level and personally motivating me.

I take this opportunity to express gratitude to all of the Department faculty members for their help and support. I also thank my parents for their encouragement and support.

Contents

Abstract 4

I.Introduction 5

II.Definition and basic properties 7

i.Non-Hermitian operators with real spectra. 7

ii.The two level PT symmetric system. 9

III.Wave diffraction in non-Hermitian lattices 12

i.PT Symmetric-Periodic Optical lattices. 12

ii.Floquet-Bloch Theory. 14

iii.Band Gap Structure. 15

iv.Orthogonality of FB modes. 19

v.Orthonormality and Projection in a Finite PT Lattice. . . . 20

vi.Wave-packet dynamics in PT crystals. 22

IV.Angular Sensitivity of Diffraction Patterns and EPs 25

i.Angular sensitivity. 25

ii.Biorthogonal Projections. 35

iii.Power Oscillations. 37

V.Conclusion and outlook 39

References 40

Abstract

Quite recently PT symmetry flooded the field of optics gaining attraction of both experimentalists and theorists alike. The outcome was the experimental demonstration of phenomena that could not been realized in standard Hermitian or conservative systems. Nowadays, the field of complex photonics is in the frontline including ideas such as unidirectional invisibility and non-reciprocal light propagation. Another notion, which was put forward was the construction of meticulous designs including both optical gain and loss regions in combination with the process of index guiding. When this concept is applied to periodic arrangements consisting of PT symmetric cells, we can get an entirely new paradigm of materials with unique characteristics. In the context of this thesis, the non-orthogonality of the eigenmodes of such systems and the beam dynamics are investigated in detail with respect to the scientific research of Kostantinos G.Makris Ramy El-Ganainy and Demetrios N.Christodoulides, PT symmetric optical lattices, *Physical Review Letters* A 81,063807(2010)[1] and K.G.Makris, R.El-Ganainy, D.N.Christodoulides, Beam dynamics in PT Symmetric Optical Lattices, *Physical Review Letters* 100,103904 (2008)[2]. *Particularly, we investigate the angular sensitivity of the diffraction pattern in a PT symmetric optical lattice under wide beam excitation near the exceptional point. Besides the fundamental importance of the characteristics of the waveguide arrays where the entire structure obeys the parity-time symmetry, angular sensitivity offers a fertile ground for potential applications, such as ultrasensitive sensors.*

I.Introduction

Symmetries are the fundamental keys in our efforts of unraveling nature's mechanisms, as they are responsible for a series of important physical phenomena we observe. Parity ($\mathcal{P}$) and time reversal ($\mathcal{T}$) symmetries have already played a crucial role in the quantum field theories. Recently, what was considered as almost "axiomatic" - the basic principle of quantum mechanics "that every observable quantity is described by a Hermitian operator", was reexamined with the discovery of non Hermitian operators with entirely real spectra as a direct result of $\mathcal{PT}$ symmetry. The last fifteen years great progress has been made with the introduction of pseudo-Hermitian operators with special symmetries and purely real spectra and led to the extension of quantum mechanics governed by non Hermitian, but $\mathcal{PT}$ symmetric operators[3].

The general concept of $\mathcal{PT}$ symmetry had a great impact in diverse areas of physics, such as quantum field theories, non-Hermitian Anderson models, lattice QCD theories, wave scattering from complex periodic potentials, just to name a few[2]. Especially in optics and integrated photonics it has been suggested that $\mathcal{PT}$ related concepts can be realized and tested thoroughly. Primarily because of the formal equivalence between the quantum mechanical Schrödinger equation and the optical wave diffraction, in conjunction with the ability to manipulate loss, gain and the process of index guiding in the same time. A Parity - Time symmetric optical media can be made through judicious inclusion of gain and loss in guided wave geometries. Linear wave propagation in such $\mathcal{PT}$ symmetric media have been investigated theoretically for the one and multi spatial dimensions. In the linear regime, new phenomena emerged; absent in Hermitian problems, such as band merging, $\mathcal{PT}$ phase transition(Exceptional Point-EP), double refraction and non reciprocal behavior[2].

These ideas stimulated the development of innovative synthetic structures and devices. Nowadays, interest in the field of $\mathcal{PT}$ symmetric optics fascinates both experimentalists and theorists alike. Cutting edge technology suggests the realization of $\mathcal{PT}$ symmetric and synthetic micro-ring lasers, observation of exceptional lines in photonic crystals among others. Moreover, notions of $\mathcal{PT}$ symmetry have greatly influenced other fields of optics and photonics such as opto-mechanics, plasmonics and metamaterials, linear and nonlinear optics[3-15].

Motivated by this recent progress, Makris *et. al* [1] investigated thoroughly the band structure and wave dynamics related to complex $\mathcal{PT}$ symmetric arrays. They demonstrated analytically and numerically the nonorthogonal nature of the corresponding Floquet-Bloch(FB) modes. Exotic, new phenomena such as double refraction, power oscillations and phase dislocations are studied in great detail.

Following Makris *et. al* research project, in my thesis I give emphasis in studying the angular sensitivity of the diffraction pattern in a $\mathcal{PT}$ symmetric optical lattice under wide beam excitation near the phase transition point(EP). This can be done by examining how intensity distribution changes, when selecting a different angle of incidence. We begin with by considering what happens under wide beam excitation to a Hermitian lattice and then compare it with the non-Hermitian case. We are looking for the appropriate angles where the system appears to be more sensitive in the Non-Hermitian case. In order to accomplish that, we imply the stationary projection coefficients, that have numerically been evaluated for the first three bands.

In the first part, we are introducing Non-Hermitian operators with real spectra and the way these ideas are used in optics today. We continue by analyzing one simple example, thus of great importance in showing the role of the phase transition points or Exceptional points(EPs), in manipulating light transport. In the second chapter, we are investigating wave propagation in linear $\mathcal{PT}$ symmetric-periodic media, Floquet-Bloch theory and the characteristics of the band structure in periodic $\mathcal{PT}$ symmetric structures. In the third chapter, we continue our analysis by deriving and analyzing the necessary conditions for the orthogonality of the FB modes and describing the FB mode properties of a finite $\mathcal{PT}$ symmetric periodic potential. It is important to note that the numerical method used is also presented. Finally, the connection between angular sensitivity and projection coefficients is described. The role of power oscillations is also highlighted in the last section.

II.Definition and basic properties

i.Non-Hermitian Operators with real spectra

Consider $\psi(\boldsymbol{r},t)$ a complex wavefunction of a quantum particle. The time dependent Schrödinger equation is:

(with $\hbar$=m=1, m stands for the mass of the particle)

$$i\frac{\partial\psi}{\partial t} = \hat{H}\,\psi(\boldsymbol{r},t) \tag{II.1}$$

where the linear operator H acts in a Hilbert space $\mathcal{H}(\mathbb{R}^D)$, $\hat{H} = \frac{\hat{p}^2}{2} + V(\hat{x})$ and $\hat{p} = -i\frac{\partial}{\partial x}$. The inner product is determined:

$$<\psi,\phi>=\int_{R^D}\psi^*(\boldsymbol{r},t)\;\phi(\boldsymbol{r},t)\,d\boldsymbol{r} \tag{II.2}$$

where D is the space dimension, ψ^* is the complex conjugate. An operator is considered Hermitian(self adjoint) if : $\hat{H}^\dagger = \hat{H}$,

$$<\hat{H}\psi,\phi =<\psi,\hat{H}\phi> \tag{II.3}$$

The two fundamental discrete symmetries in physics are Parity($\mathcal{P}$) and Time reversal($\mathcal{T}$). They are described by the Parity operator($\hat{P}$) and the Time operator($\hat{T}$).

$$\hat{P}\psi(\boldsymbol{r},t)=\psi(-\boldsymbol{r},t) \quad \text{and} \quad \hat{T}\psi(\boldsymbol{r},t)=\psi^*(\boldsymbol{r},-t) \tag{II.4}$$

The action of the Parity operator($\hat{P}$) is defined by the relations: $\hat{p}\to-\hat{p}$, $\hat{x}\to-\hat{x}$ and for the Time reversal operator($\hat{T}$) by $\hat{p}\to-\hat{p}$, $\hat{x}\to\hat{x}$ and $i\to-i$, where $\hat{p}$, $\hat{x}$ are the momentum and position operators, respectively[3].

The operator($\hat{T}$) is antilinear, moreover $P^2 = T^2 = I$, where I is the identity operator, also $[\mathcal{P},\mathcal{T}]=0$. An operator $\hat{H}$ can be defined as $\mathcal{PT}$ symmetric if $[\hat{P}\hat{T},\hat{H}]=0$. As a direct result a Hamiltonian is called $\mathcal{PT}$ symmetric, if and only if, it has the same eigenfunctions with that of the $\mathcal{PT}$ operator[3].

As mentioned $\hat{T}$ operation gives a time reversal action, so $\hat{T}\hat{H} = \frac{\hat{p}^2}{2} + V^*(\hat{x})$ then $\hat{H}\hat{P}\hat{T} = \frac{\hat{p}^2}{2} + V(\hat{x})$ and $\hat{P}\hat{T}\hat{H} = \frac{\hat{p}^2}{2} + V^*(-\hat{x})$ (II.5)[3]. A necessary but not sufficient condition for a Hamiltonian to be $\mathcal{PT}$ symmetric is $V^*(\hat{x}) = V^*(-\hat{x})$(II.6)[16].We can deduce that Parity-Time symmetry demands that the real part of the complex potential must be a symmetric function of position, while the imaginary part should be antisymmetric. $\mathcal{PT}$ symmetry does not mean that the spectrum is real, unlike Hermiticity. On the other hand, when combined with the requirement for the $\mathcal{PT}$ symmetry to be unbroken, guarantees the spectrum to be entirely real[3].

Consider E an eigenvalue of H, then $\hat{H}\psi = E\psi \xrightarrow[PT\ operator]{} \hat{H}(\hat{P}\hat{T}\psi) = E^*(\hat{P}\hat{T}\psi)$(II.7). If the $\mathcal{PT}$ symmetry of H is unbroken, $\hat{H}\psi = E^*\psi$, then E is real and the spectrum of H is purely real. Phase transitions points are where the broken $\mathcal{PT}$ symmetry occurs, and are closely related with the appearance of complex eigenvalues in the spectrum of H, as the Hamiltonian and the $\mathcal{PT}$ operator now, do not have the same set of eigenfunctions(even though they commute)[3]. In this case, also called pseudo Hermitian regime, the eigenfunctions are no longer orthogonal, $< m|n > \neq \delta_{m,n}$ and the vector space is considered "skewed".

These ideas can easily been applied in optics in the base that include both optical gain and loss judiciously in regions and the process of index guiding. Thinking the complex refractive index as an optical potential, for example $\mathrm{V}(x) = n_R(x) + in_I(x)$. Of course in optical systems $\mathcal{PT}$ symmetry requires that $n_R(x) = n_R(-x)$ and the imaginary part which represents either gain or loss is an antisymmetric function of position, $n_I(x) = -n_I(-x)$ [2] .

ii.The two level PT symmetric system

In optics this simple example depicts two coupled resonators or waveguides, one experiences gain and at the same time the other has the same amount of loss. The example presented describes a coupled waveguide arrangement, and in this case energy exchange takes place in space. This example depicts the role and importance of the phase transition points or Exceptional points(EPs), in manipulating light transport. At first we present an eigenvalue analysis of the problem and then follows a comparison between the numerical and the analytical method.

Field evolution dynamics of the PT coupler is described by:

$$i\frac{da}{dz} + kb - iga = 0$$

$$i\frac{db}{dz} + ka + igb = 0 \quad \text{(II.8)}$$

α and b represent the modal field amplitudes, g stands for the gain or loss coefficient and k is the coupling strength. After rearranging (II.8), we get the following:

$$-i\frac{d}{dz}\begin{pmatrix} a \\ b \end{pmatrix} = \begin{pmatrix} -ig & k \\ k & ig \end{pmatrix}\begin{pmatrix} a \\ b \end{pmatrix} \quad \text{(II.9)}$$

The stationary solutions are: $\begin{pmatrix} a \\ b \end{pmatrix} = \begin{pmatrix} u \\ v \end{pmatrix} e^{i\lambda_{1,2}\, z}$. The system supports two supermodes with distinct characteristics that rely upon the ratio between gain and loss coefficient and coupling strength, parameters g and k respectively.

When $\frac{g}{k} < 1$, the eigenvalues are $\lambda_{1,2} = \pm cos\theta$, where the parameter θ is defined as: $\theta = \sin^{-1}(\frac{g}{k})$ and $\frac{g}{k} = sin\theta$. In this case the two eigenvalues are real and the corresponding eigenvectors are $|1> = \begin{pmatrix} 1 \\ e^{i\theta} \end{pmatrix}$ and $|2> = \begin{pmatrix} 1 \\ -e^{-i\theta} \end{pmatrix}$. These eigenvectors are not orthogonal despite the fact that the corresponding spectrum is real.

However, when gain or loss coefficient has a greater value than the coupling strength $\frac{g}{k} > 1$, the eigenvalues are $\lambda_{1,2} = \mp isinh\theta$, where the parameter θ is defined as: $\theta = \cosh^{-1}(\frac{g}{k})$ and $\frac{g}{k} = cosh\theta$. Now the corresponding non-orthogonal eigenvectors are $|1> = \begin{pmatrix} 1 \\ ie^{-\theta} \end{pmatrix}$ and $|2> = \begin{pmatrix} 1 \\ ie^{\theta} \end{pmatrix}$. The symmetry of each mode is broken, one of the eigenmodes is in the "gainy" channel, and in the mean time the other is in the "lossy" channel, while the two channels are coupled.

The transition point, where $\frac{g}{k} = 1$, between the broken and unbroken symmetry regime is called the exceptional point(EP). In the EP the two eigenvectors turn to be exactly identical, $\binom{1}{i}$. The Cauchy–Schwarz inequality allows one to extend the notion of "angle between two vectors" to any real inner product space, by defining:

$$cos\ \theta_{1,2} = \frac{\langle 1,2 \rangle}{\|1\|\|2\|} \qquad \text{(II.10)}$$

Hilbert spaces are simply generalizations of the Euclidean space. In order to define an angle in complex inner product spaces, we take the real part of the eigenvectors. In our case, θ_λ equals zero, given that the two eigenvectors are exactly identical. Neither one oscillates nor experiences exponential variation. In other words, the dimensionality of the vector space is suddenly decreased. $\mathcal{PT}$ symmetry phase transition was first made possible to observe in coupled optical elements.

Actually the first $\mathcal{PT}$ symmetric experimental setup included both gain and loss in two coupled channels etched in a photorefractive lithium niobate ($LiNbO_3$) crystal. In this system gain was equipped via two wave mixing. In Fig.1 the first $\mathcal{PT}$ symmetric experimental setup is depicted.

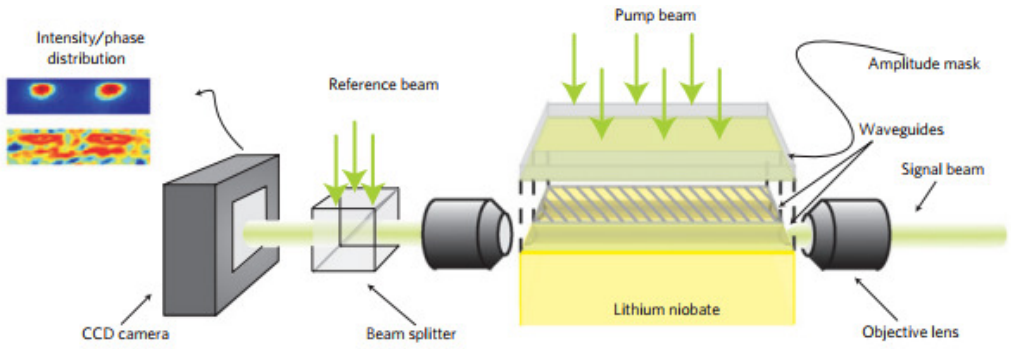

Fig.1: First $\mathcal{PT}$ symmetric experimental setup including both gain an loss in two coupled wave channels[17].

In a next step, we demonstrated the Real and Imaginary Parts of the eigenvalues versus gain-loss to coupling ratio, computed both numerically and analytically(Figs.2 (a),(b)). In order to compare the two methods followed, we computed the absolute difference of the eigenvalues we found numerically and analytically. In this case they agree, in the 10^{-15} digit(Fig.2(c)).

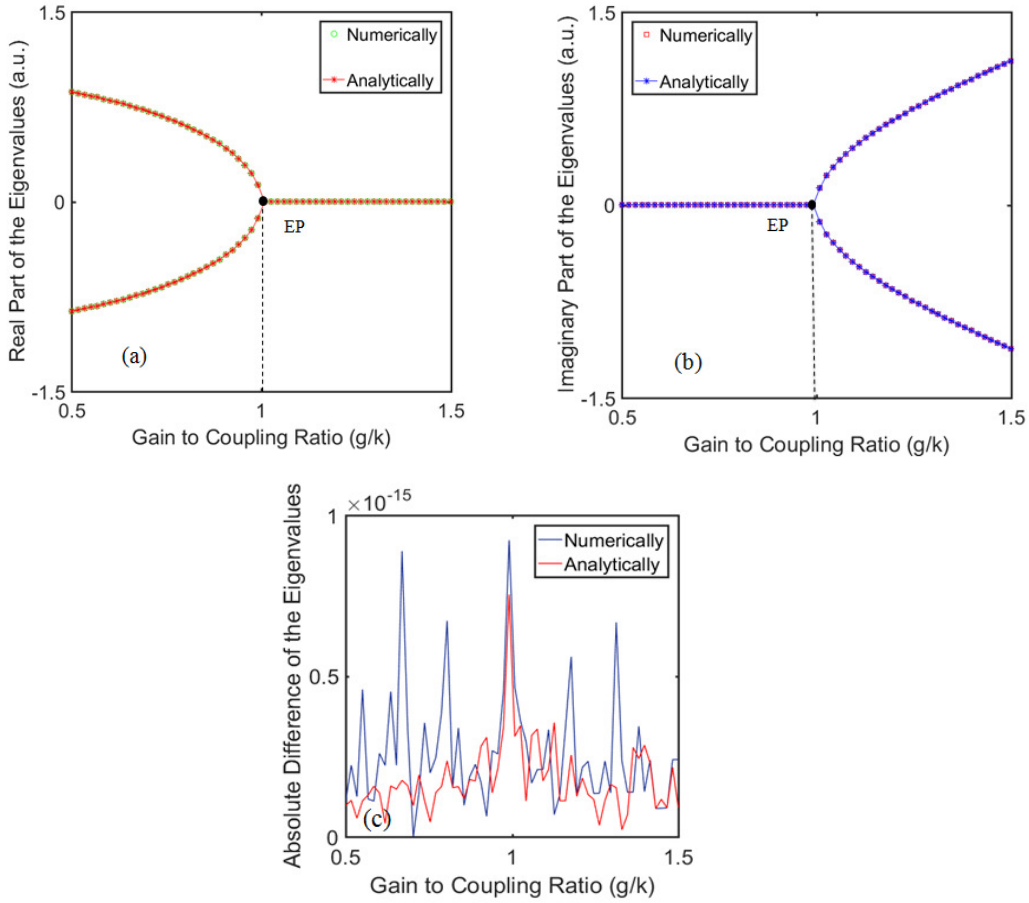

Figs.2 (a),(b),(c): (a) Real part of the eigenvalues versus gain-loss to coupling ratio. The red solid line(Analytically) is perfectly fitted with the green dotted(10^{-15}). (b) Imaginary part of the eigenvalues versus gain-loss to coupling ratio. Again the level of agreement is at the 10^{-15} digit(analytically blue solid line, numerically red dotted line). After the exceptional point g/k =1, one of the supermodes is amplified, while the other one is in a dissipative regime. (c) Quantitative comparison of the analytical and numerical method in an absolute difference of the eigenvalues versus gain to coupling ratio diagram.

III.Wave diffraction in non-Hermitian lattices

i.PT Symmetric Periodic Optical Lattices

$\mathcal{PT}$ related concepts can be realized and studied experimentally. Mainly due to the formal equivalence between the quantum mechanical Schrödinger equation and the optical diffraction equation. In this section we discuss the analogy between quantum mechanics and optics and the fact that they share the same mathematical formalism. We shed light on the spatial domain, especially optical beam propagation in $\mathcal{PT}$ symmetric complex potentials. In order to fully understand the properties of a periodic $\mathcal{PT}$ structure we later on, analyze its corresponding band structure. As we have already mentioned, these $\mathcal{PT}$ optical potentials can be realized when gain and loss regions can be combined with the involvement of the index guiding. Given the fact, that the complex refractive index distribution $n(x) = n_o + n_R(x) + in_I(x)$,can be seen as an optical potential, thus it is possible to realize a $\mathcal{PT}$ symmetric system that obeys $n_R(x) = n_R(-x)$ and $n_I(x) = -n_I(-x)$. n_o is the background refractive index, $n_R(x)$ is the real index profile of the lattice, $n_I(x)$ describes the gain or loss distribution of the structure (practically $n_o \gg n_{R,I}(x)$). This means that the refractive index must be an even function of position, while the gain/loss distribution should be odd. The periodicity of the $\mathcal{PT}$ symmetric potential is satisfied under the condition: $n_{R,I}(x) = n_{R,I}(x + D)$, D is the period of the optical lattice[17].

Wave propagation in linear $\mathcal{PT}$ symmetric-periodic Media

More specifically, the equation governing optical beam propagation is defined by a Schrödinger-like equation, the Paraxial Equation of Diffraction, in physical units.

$$iU_z + \frac{1}{2k_o n_o} U_{xx} + k_o[n_R(x) + in_I(x)]U = 0 \qquad \text{(III.1)}$$

where U, is the electric field of the beam that obeys the paraxial equation of diffraction z is the propagation distance, x stands for the spatial coordinate and k_o=2π/λ_o , also k=$k_o n_o$ with λ_o being the light wavelength and n_o is the background refractive index[2].

However, in order for these $\mathcal{PT}$ symmetric lattices to be realized the parameters described above can take only specific values. For example, the light wavelength in the visible and in the long wavelength regime varies from $0.5\mu m$ to $1.6\mu m$, using a periodic index modulation of the order of ${\Delta n_R}^{max} \approx 10^{-3}$ with $D \approx 10 - 20\mu m$, very closely to real arrays, while the gain or loss maximum values are $g = -a \approx 30cm^{-1}$ or ${\Delta n_I}^{max} \approx 5 \cdot 10^{-4}$[18] . These values for the gain and loss coefficients can be achieved using quantum well lasers, or photorefractive structures through two

wave mixing[19]. Now by defining, $\xi = \frac{z}{2k_o {x_o}^2}$, $\eta = \frac{x}{x_o}$, where x_o is an arbitrary scaling factor.

By applying these transformations to (III.1) we derive the following :

$$i\frac{\partial U}{\partial \xi} + \frac{\partial^2 U}{\partial \eta^2} + [2k{x_o}^2 k_o]\,(n_R(x) + in_I(x))\,U = 0 \qquad \text{(III.2)}$$

We choose x_o, so that $2k{x_o}^2 k_o \max(n_R) = 1$. The normalized paraxial

equation of diffraction now is : $i\frac{\partial U}{\partial \xi} + \frac{\partial^2 U}{\partial \xi^2} + V(\eta)U = 0$ (III.3)

where $V(\eta) = V^*(-\eta)$ and $V(\eta) = 2{k_o}^2 {x_o}^2 n_o\,[n_R(\eta) + in_I(\eta)]$.

And the physical period of $cos^2(\eta) = cos^2(\frac{x}{x_o})$ is $D = \pi\, x_o$ so, $x_o = \frac{D}{\pi}$.

In the next step we are rewriting equation (III.2), in normalized units again but we have substituted η, ξ to correspond to the physical units spatial coordinate and propagation distance respectively. Finally we get the normalized equation of diffraction in a lattice:

$$i\frac{\partial \psi}{\partial z} + \frac{\partial^2 \psi}{\partial x^2} + V(x)\psi = 0 \qquad \text{(III.4)}$$

ψ represents the electric field amplitude, $V(x)$ is the complex periodic optical potential with period D, $V(x) = V(x + D)$. This complex potential is a $\mathcal{PT}$ symmetric potential given the fact that its real part or refractive index profile is an even function of x and the loss/gain profile is antisymmetric, that means $V(x) = V^*(-x)$.

The optical power is defined as: $P(z) = \int_{-\infty}^{+\infty} |\psi(x,z)|^2\, dx$. However, the actual total power is not conserved. Its evolution in place (z coordinate):

$$\frac{dP(z)}{dz} = -2\int_{-\infty}^{+\infty} Im\,[V(x)]|\psi(x,z)|^2\, dx \qquad \text{(III.5)}$$

$\mathcal{PT}$ symmetric optical lattices may have purely real spectrum and judiciously distributed gain and loss, however remains their behavior remains a subject of discussion. As outlined by Berry[20],[21], the diffraction of optical beams in $\mathcal{PT}$ periodic potentials is not unitary and the power is not conserved. This "power oscillation" effect derives from the non-orthogonality of the eigenmodes of any $\mathcal{PT}$ symmetric non-Hermitian system[1],[2]. Power oscillations are discussed in Chapter VIII. In the next section we discuss the properties of a Periodic $\mathcal{PT}$ structure, starting with Floquet-Bloch theory and Band gap structure.

ii.Floquet-Bloch Theory

The properties of a periodic $\mathcal{PT}$ structure are tightly bonded with its corresponding band structure. In order to analyze it, we seek to find solutions of the form:

$$\psi(x,z) = \phi(x)e^{i\beta z} \tag{III.6}$$

where β is the eigenvalue(propagation constant) and $\phi(x)$ is the eigenmode that appears in:

$$\left[\frac{d^2}{dx^2} + V(x)\right]\phi = \beta\phi \tag{III.7A}$$

Equation (III.4) is a second order differential equation, with $V(x)$ being a complex periodic potential. In this case the two independent solutions as directed by Bloch theory[18,22,23]: $\phi_n^{(1)}(x,k)=u_n^{(1)}(x,k)e^{ikx}$ and $\phi_n^{(2)}(x,k)=u_n^{(2)}(x,k)e^{-ikx}$, (III.7B)

where n ϵ Z^+, $k = k(\beta)$ the Bloch momentum and $u_n^{(1),(2)}(x,k)$ are complex periodic and bounded functions of x. And must satisfy the following,

$$\left[\left(\frac{d}{dx} \pm ik\right)^2 + V(x)\right] u_n^{(1)}(x,k) = \beta_n(k)\, u_n^{(1),(2)}(x,k) \tag{III.8A}$$

$$u_n^{(1),(2)}(x+D,k) = u_n^{(1),(2)}(x,k),\ k \epsilon \left[-\frac{\pi}{D}, \frac{\pi}{D}\right] \tag{III.8B}$$

Moreover, only one set of solutions is necessary to satisfy equation (III.7A), for this reason we write them as: $\phi_n(x,k) = u_n(x,k)\, e^{ikx}$ (III.9) also the necessary periodicity condition $u_n(x+D,k) = u_n(x,k)$. Now $u_n(x,k)$ has to satisfy,

$$\frac{d^2u_n(x,k)}{dx^2} + 2ik\frac{du_n(x,k)}{dx} + [V(x) - k^2]u_n(x,k) = \beta_n(k)\, u_n(x,k) \tag{III.10}$$

Nevertheless, the computation of the complex conjugate of (III.10), with the necessary changes in variables such as x→ −x, $k \to -k$ and by using the necessary condition for the $\mathcal{PT}$ symmetric potential $V(x) = V^*(-x)$,

$$\frac{d^2u_n^*(-x,-k)}{dx^2} - 2ik\frac{du_n^*(-x,-k)}{dx} + [V(x) - k^2]u_n^*(-x,-k) = \beta_n^*(-k)u_n^*(-x,-k)$$

marked as equation (III.11), leads us in two substantially different cases.

In the first case we are dealing with Real potentials, here $Im[V(x)] = 0$. While the spectrum of $\left[\frac{d^2}{dx^2} + V(x)\right]$ is real and contains spectral bands, separated from infinite spectral gaps[24-26]. Thus the corresponding eigenfunctions are given by (III.9). What is crucial is that when $\beta(k)$ is real, then is a bounded function of x, thus it corresponds to a spectral band. Hence, when $\beta(k)$ is imaginary it belongs to a

spectral gap. In our field of expertise, and generally in optics, $\beta(k)$ is related to as photonic band gap.

We can calculate by numerically computing equation (III.10) and take into account the periodic boundary condition on the primitive cell of the lattice. Because of the time-reversibility the band gap structure is symmetric around $k = 0$, for example $\beta_n(k) = \beta_n(-k)$. One-dimensional periodic potentials have infinitely many gaps, and in optics it is mentioned as a complete band gap. The final step for our analysis is the orthogonality relation that the Floquet-Bloch functions have to comply with:

$$\int_{-\infty}^{+\infty} \phi_m^*(x,k')\phi_n(x,k)dx = \delta_{n,m}\,\delta(k-k') \qquad \text{(III.12)}$$

In the second case, we are investigating complex potentials, $Im[V(x)] \neq 0$, the Floquet-Bloch theorem is still valid. Its corresponding eigenfunctions are again given by (III.9), with the complex now $u_n(x,k)$ with correspondence to equation (III.10). The fact that in this case the spectral problem is not self-adjoint, affects also the band structure that is not generally real. We should not forget that the $\mathcal{PT}$ symmetric condition $V(x) = V^*(-x)$ gives indications for the reality of the spectrum[27-31]. Specifically, if $[\beta_n(k), \phi_n(x,k)]$ stands for a spectral pair of $\left[\frac{d^2}{dx^2} + V(x)\right]\phi = \beta\phi$, with complex $\beta_n(k)$, then we have $[\lambda_n{}^*(k), \phi_n{}^*(-x,-k)]$. Hence, in the case of complex potentials, FB modes cannot satisfy relation (III.12) for orthogonality, but a different relation of the type(as we demonstrate in Chapter VIII):

$$\int_{-\infty}^{+\infty} \phi_m^*(-x,-k')\phi_n(x,k)dx \propto \delta_{n,m}\,\delta(k-k') \qquad \text{(III.13)}$$

iii.Band Gap Structure

At first, without any loss of the generality, we consider the periodic $\mathcal{PT}$ potential of the form:

$$V(x) = 4[cos^2 x + iV_o \sin(2x)] \qquad \text{(III.14)}$$

with period D=π for both real and imaginary parts, V_o is a real constant that can be chose to be non negative. Once again the condition $V(x) = V^*(-x)$ satisfied by the potential above is a necessary but not a sufficient condition for the reality of the spectrum. Furthermore, we can find out by spectral methods numerically a $\mathcal{PT}$ threshold(V_o^{th}). Below this threshold, all the propagation eigenvalues for every band and every Bloch wave number k are real. On the other hand above the $\mathcal{PT}$ threshold a sudden phase transition takes place[32-35]. Consequently, the spectrum is partially complex notwithstanding the condition for the $\mathcal{PT}$ symmetric potential $V(x) = V^*(-x)$, which is a necessary but not a sufficient condition for the reality of the spectrum.

For this specific potential numerical computations have determined the threshold of $V_o^{th} = 0.5$ .Concerning the way it affects the band structure, for V_o <0.5 the band structure is entirely real, on the other hand for V_o >0.5 the band structure becomes partially complex. At first, we investigate the case for V_o =0.0, that means our problem is now Hermitian. In Fig.3(a), is presented the band diagram for V_o =0.0 (Hermitian case) and V_o =0.25 (Non-Hermitian case). In the next step(Non-Hermitian case), we present the real and the imaginary part of the potential(III.14) for two cases when, V_o =0.25 and V_o =0.5, Fig.3(b),(c) respectively.

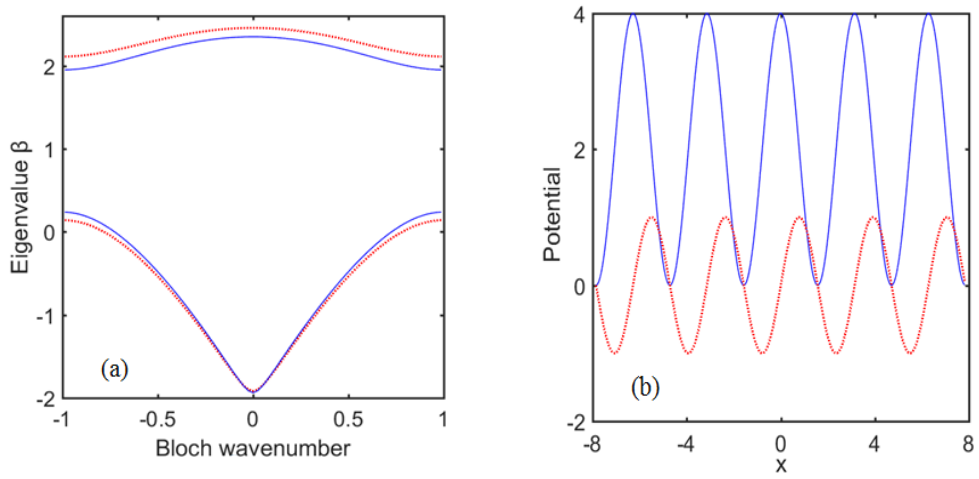

Figs.3(a),(b):(a)Band structure of a Hermitian lattice(red dotted line), and the corresponding band structure of a $\mathcal{PT}$ symmetric lattice with V_o =0.25(blue solid line). Please note the differences in the forbidden gaps for a specific value of V_o, in the Non-Hermitian case compared with the Hermitian case. (b)Real(blue solid line) and imaginary(red dotted line) part of a $\mathcal{PT}$ symmetric lattice with V_o =0.25.

We give emphasis in highlighting the changes in the band structure below and above the $\mathcal{PT}$ symmetry breaking threshold (V_o^{th} =0.5) . Figure 4(a) depicts the first two bands of the potential we investigate when V_o =0.25 and V_o =0.5 . At this point, it is important to take into account that below the V_o^{th} =0.5 all the forbidden gaps in the band structure are open. On the other hand, when V_o^{th} =0.5 the first gap at the edges of the Brillouin zone $k = \pm 1$ closes. As shown in Figs4(b),(c) , when we are studying the band structure above the $\mathcal{PT}$ symmetry breaking threshold, it is evident that the first two bands are merging. It is important to note that the spectrum turns to be complex above the critical values of the threshold and initiates from the lowest bands.

The result is oval shaped, a double valued band, that also corresponds to the complex spectrum. The real and the imaginary components of this band are presented in these figures. The propagation eigenvalues are completely real in the double valued regions, whereas in the regions fold over each other, they form complex conjugate pairs.

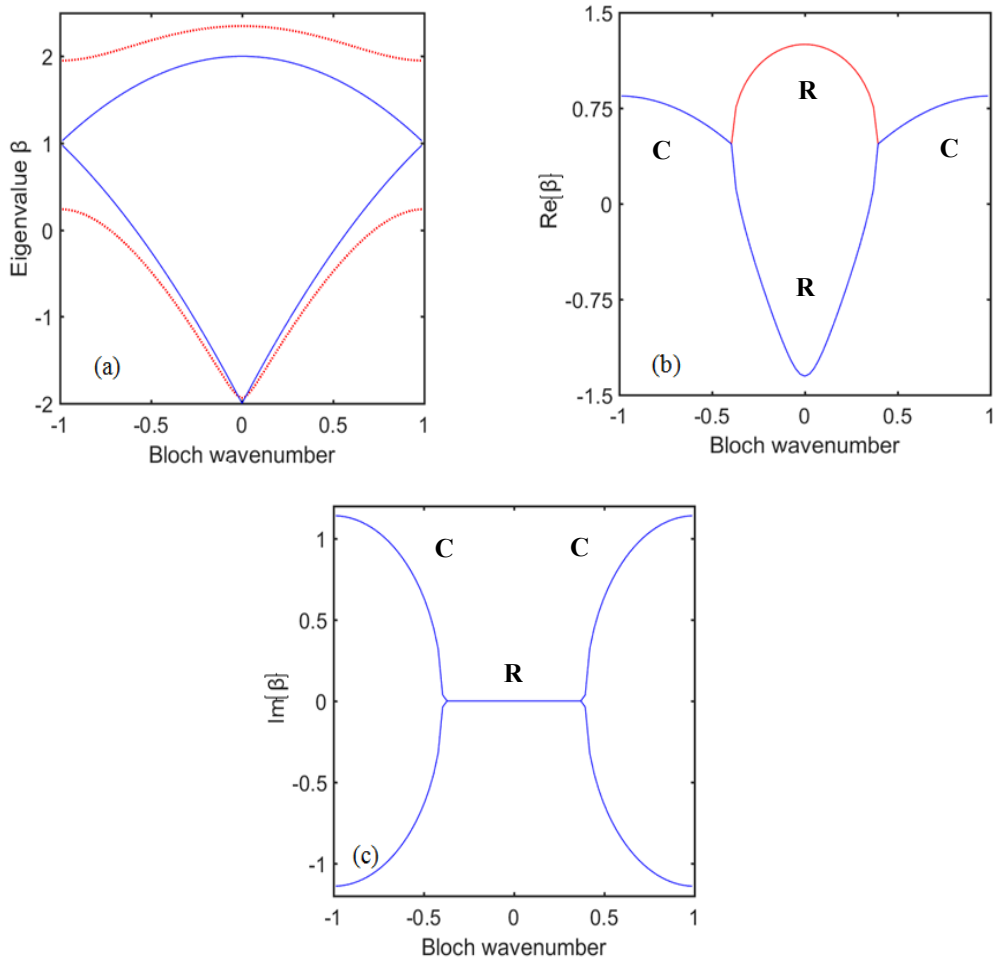

Figs.4(a),(b),(c):(a)The real part of the first two bands obtained for different values of gain/loss amplitude V_o =0.25(red dotted line) and V_o = 0.5(blue solid line). It is important to highlight the merge of the first and the second band for V_o =0.5, forming an oval shaped band.(b)Real part of the first two bands for V_o =0.75.(c)The corresponding imaginary component of the bands as presented in (b).

As mentioned above after crossing the critical value, the spectrum gradually becomes complex, while the first two bands merge shaping an oval, the rest of the bands continue to have real eigenvalues. As shown below in Figure 5, when the interest of study is the rest of the bands(such as the third and the fourth), for V_o exceeding the first threshold, Makris *et al* have noted the existence of another secondary threshold, that leads to the merge of the third and the fourth band as well.

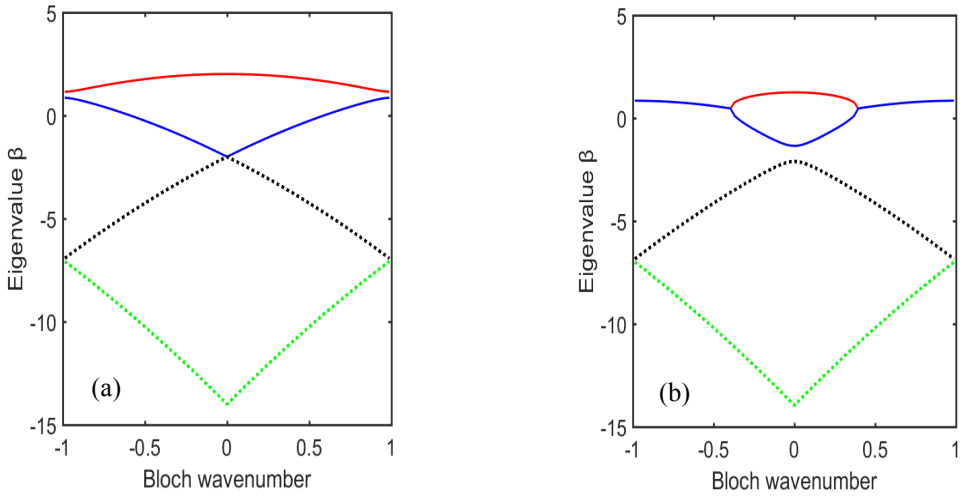

Fig5: The real part of the first four bands of the same potential for (a) V_o=0.495 and (b) V_o=0.75 . The first and the second band(solid line) are merged, while the third(black dotted line) and the fourth green(dotted line) are also depicted.

iv.Orthogonality of FB modes

In this section we investigate the orthogonality of FB modes in $\mathcal{PT}$ symmetric periodic potentials thoroughly. We determine the inner product algebra for $\mathcal{PT}$ periodic potentials, the orthogonality in a single $\mathcal{PT}$ cell and the orthonormality and projection in a finite $\mathcal{PT}$ Lattice[1],[2].

Inner products

In standard Hermitian optics when $V(x)$ is real two different FB modes $\phi_n(x,k)$, $\phi_m(x,k')$ satisfy the orthogonality relation

$$\int_{-\infty}^{+\infty} \phi_m^*(x,k')\phi_n(x,k)dx = \delta_{n,m}\,\delta(k-k'), \qquad \text{(III.15)}$$

with accordance to the inner product $\langle f,g\rangle=\int_{-\infty}^{+\infty} f(x)^*\,g(x)dx$ (III.16),where $f(x)$ and $g(x)$ are two functions with complex values. The inner product for a complex $\mathcal{PT}$ symmetric lattice is given by:

$$\{f(x,k),g(x,k)\} = \int_{-\infty}^{+\infty} f^*(-x,-k)\,g(x,k)\;dx \qquad \text{(III.17)}$$

The inner product in our case dissent from the inner product in the real lattice. Thus, the orthogonality condition is going to have a different form as well.

Orthogonality in a Single $\mathcal{PT}$ Cell

In order to determine the orthogonality condition first we must consider the orthogonality in a single cell, in a finite lattice and at the end the case for an infinite lattice[1]. Always our eigenvalue problem refers to equation (III.10). However, in the context of this thesis orthogonality in a single $\mathcal{PT}$ cell and a finite lattice is presented and we assume the logical generalization in an infinite lattice. In this paragraph we present the orthogonality condition in one individual cell of the periodic potential, in the range $\left[-\frac{D}{2},\frac{D}{2}\right]$. Assume two FB modes $u_{kn}(x,k)$ and $u_{km}(x,k)$, corresponding to different bands($n\neq m$) with the same Bloch wave number. Moreover, the potential $V(x)$ is below the $\mathcal{PT}$ phase transition point, so the spectrum is considered to be purely real. The normalized FB modes can be defined as:

$$\Phi_n(x,k)\equiv\frac{\phi_n(x,k)}{\sqrt{c_{kn}}},\; U_n(x,k)\equiv\frac{u_n(x,k)}{\sqrt{c_{kn}}} \text{ and } c_{kn}\equiv\int_{-D/2}^{+D/2}\phi_n^*(-x,-k)\,\phi_n(x,k)\,dx$$

highlighted as equations (III.18). c_{kn} is a unique normalization coefficient for every FB mode, that solely depends on the band index n and the Bloch wave number k. Hence, we must outline that c_{kn} are in principle complex valued numbers and thus satisfy the relation $c_{kn}=c_{-kn}{}^*$.

The final orthogonality condition is [31]:

$$\int_{cell} \Phi_m{}^*(-x,-k)\Phi_n\,(x,k)\;dx = d_{kn}\delta_{n,m} \tag{III.19}$$

where,

$$d_{kn} \equiv \begin{cases} 1, & \text{when } c_{kn} \in \mathbb{C} \text{ or } c_{kn} > 0 \\ -1, & \text{when } c_{kn} < 0 \end{cases}$$

$\delta_{n,m}$ is the Kronecker delta. Makris et *al.* in their work have numerically tested that for all FB modes below the $\mathcal{PT}$ phase transition point $c_{kn} \neq 0$. Since there are no self-orthogonal FB modes in this problem, the above normalization is well defined[25].

v.Orthonormality and Projection in a Finite PT Lattice

The aim of this paragraph is to highlight the FB mode properties of a finite $\mathcal{PT}$ symmetric periodic potential where periodic boundary conditions are applied at the endpoints of the lattice. With this practice we can numerically calculate the corresponding projection coefficients. The singularities of Dirac functions in the orthonormality condition in an infinite $\mathcal{PT}$ lattice as a complete approach suggests, are not there anymore and have been replaced by a Kronecker delta. In the limit $N \to \infty$ the results approach that of the infinite lattice.

This is a typical approach when we are studying periodic crystals in solid state physics[1],[2]. We should first consider a finite lattice with N cells, and $L = ND$. K.G.Makris *et al* in PT symmetric optical lattices[1], have meticulously described the FB properties of a finite $\mathcal{PT}$ symmetric periodic potential as mentioned above and deducted that the formulas for the projections coefficients and the Parseval's identity equations (III. 20) and (III. 21) respectively assuming that an arbitrary optical beam $f(x,z)$ can be expanded in terms of the finite number of FB modes.

$$A_{n,k_m} = d_{n,k_m} e^{-i\beta_n(k_m)z} \int_{\substack{finite \\ lattice}} \Phi_n{}^*(-x,-k')f(x,z)\,dx \tag{III. 20}$$

$$\int_{\substack{finite \\ lattice}} f^*(-x,z)\,f(x,z)\,dx = \sum_{n=1}^{+\infty} \sum_{m=-N'}^{N'} d_{n,k_m}\, A_{n,k_m} A^*_{n,k_m} \tag{III. 21}$$

This approach allows us to numerically verify all the relations, since the spectrum in the k-space is discrete and has a finite number of FB modes. Therefore, we can express any beam profile as a linear superposition of FB modes[1]. By this, we can determine the energy content of the beam in every transmission band. In the next chapters the dynamics as well as the propagation characteristics of optical beams in $\mathcal{PT}$ periodic potentials are investigated in detail. It is important to highlight, that all the numerical results in the next chapters concerning Beam dynamics, Non-orthogonal Projections and Power Oscillations have been acquired by using in all three cases a finite lattice.

vi.Wavepacket dynamics in PT crystals

In this section we discuss important issues related to the numerical analysis and procedure followed to describe Beam dynamics and especially Angular Sensitivity, as it will be presented in the following chapters.

The Nonlinear Schrödinger equation(NLSE) is an optical potential $V(x,y)$ under an initial excitation $f(x,y)$, in a normalized form generally, is given by:

$$i\frac{\partial\psi}{\partial z}+\frac{\partial^2\psi}{\partial x^2}+\frac{\partial^2\psi}{\partial y^2}+V(x,y,z)\psi+|\psi|^2\psi=0 \qquad \text{(III.22)}$$

where the first term $i\frac{\partial\psi}{\partial z}$ describes evolution dynamics, the terms $\frac{\partial^2\psi}{\partial x^2}$, $\frac{\partial^2\psi}{\partial y^2}$ represent diffraction, $V(x,y,z)$ is an optical potential and $|\psi|^2$ is the Kerr Nonlinearity. The condition for the initial excitation is $\psi(x,y,0)=f(x,y)$.

The above problem cannot be solved analytically in the general case for a given potential V and a given function f. For this reason, we have to use numerical methods. Beam Propagation Method(BPM) is any numerical method solving the initial value problem as described above. The Nonlinear Schrödinger equation(NLSE) in an 1D optical potential $V(x)$ under the excitation $f(x)$ in normalized units is the following:

$$i\frac{\partial\psi}{\partial z}+\frac{\partial^2\psi}{\partial x^2}+\frac{\partial^2\psi}{\partial y^2}+V(x,y,z)\psi+|\psi|^2\psi=0 \qquad \text{(III.23)}$$

$$\psi(x,0)=f(x)$$

Spectral Method

The method we choose to solve the general problem is the *Spectral Method or method of Integrating Factors*. The basic idea of this method lies in applying a suitable transformation in order to eliminate the linear part of the partially differential equation in the Fourier domain. As we can see, the problem from a nonlinear partial differential equation has been transformed to a nonlinear ordinary differential equation. Now it can be easily computed by numerical integration methods, such as Runge-Kutta method. This transformation applied is an assumed solution of a specific form, that refers to the solution of the linear diffraction problem.

$\underbrace{i\frac{\partial\psi}{\partial z}+\frac{\partial^2\psi}{\partial x^2}=0}_{\textit{Linear problem}}$, while the exact solution is $\psi(x,z)=\underbrace{\int_{-\infty}^{+\infty}\tilde{\psi}(p,z_o)e^{-ik^2z}\,e^{i(2\pi px)}dp}_{\textit{Independent of } z}$,

nothing else than, a superposition of plane waves.

In the next step, we seek to find a way to express the second order PDE as one or more uncoupled first order ODEs. In our problem this has the to do with approximating the solution of the nonlinear problem as a superposition of orthogonal modes, with an amplitude u dependent of z. We consider that the solution of the nonlinear problem can be expressed as superposition of plane waves, with an amplitude dependency of z. We have to note here, that there is no approximation.

$\underbrace{i\frac{\partial\psi}{\partial z}+\frac{\partial^2\psi}{\partial x^2}+\frac{\partial^2\psi}{\partial y^2}+V(x,y,z)\psi+|\psi|^2\psi=0}_{Nonlinear\ problem}$,while the assumed solution is given by:

$\underbrace{\psi(x,z)=\int_{-\infty}^{+\infty}\tilde{u}(p,z)e^{-ik^2z}\,e^{i(2\pi px)}dp}_{z\ dependent}$.

This method is defined as spectral because, the problem is solved numerically in Fourier space and then we take the transformation of the acquired solution to the real space.

Fourier pairs are defined by: $F\{\psi(\mathrm{x},\mathrm{z})\}=\phi(\mathrm{p},\mathrm{z})=\int_{-\infty}^{+\infty}\psi(\mathrm{x},\mathrm{z})\mathrm{e}^{-\mathrm{i}2\pi px}\,\mathrm{dx}$ as well

as by $\psi(\mathrm{x},\mathrm{z})=\int_{-\infty}^{+\infty}\tilde{\psi}(\mathrm{p},\mathrm{z})\mathrm{e}^{\mathrm{i}2\pi px}\,\mathrm{dp}$. (III.24)

The solution for the linear problem is the following: $\tilde{\psi}(\mathrm{p},\mathrm{z})=\tilde{\psi}(p,z_o)e^{-ik^2z}$ where $k=2\pi p$.

Now for the Nonlinear problem we have: $F\left\{\frac{\partial\psi}{\partial z}\right\}=F\left\{i\frac{\partial^2\psi}{\partial x^2}+i\,V(x)\psi+i|\psi|^2\psi\right\}\Rightarrow$

$\Rightarrow\frac{\partial\tilde{\psi}}{\partial z}=-ik^2\tilde{\psi}+\ F\{iV(x)\psi+i|\psi|^2\psi\}$ (III.25)

If we consider a solution of the form:

$\left(\psi(x,z)=\int_{-\infty}^{+\infty}\tilde{u}\,(p,z)e^{-ik^2z}\,e^{i2\pi px}\ dp\right)\xrightarrow{\mathcal{F.T.}}\tilde{\psi}(p,z)=\tilde{u}(p,z)e^{-ik^2z}$

From equation (III.25), we derive the following:

$\frac{\partial\tilde{u}}{\partial z}e^{-ik^2z}-ik^2z\,\tilde{u}\,e^{-ik^2z}=-ik^2z\,\tilde{u}\,e^{-ik^2z}+F\{iV(x)\psi+i|\psi|^2\psi\}$, so we finally get: $\frac{\partial\tilde{u}}{\partial z}=ie^{ik^2z}\,F\{V(x)\psi+|\psi|^2\psi\}$ (III.26), we should not forget that :

$\psi(x,z)=F^{-1}\left[\tilde{u}(p,z)e^{-ik^2z}\right]$ (III.27), so we derive the exact result:

$\frac{\partial\tilde{u}}{\partial z}=\ ie^{ik^2z}\,F\left\{\left[\,V(x)+\left|F^{-1}\left[\tilde{u}\,e^{-ik^2z}\right]\right|^2\right]\ F^{-1}\left[\tilde{u}\,e^{-ik^2z}\right]\right\}$ (III.28)

All the results derived are in terms of continuous Fourier transforms. In order to compute these transforms numerically we should introduce them to the discrete domain. The way to performed it, is by using Discrete Fourier Transform(DFT). It is important to note that in the context of this thesis the systematically discretization analysis has been skipped. To continue with, we present the basic discretizations concerning space and frequency respectively.

Space discretization

$$x_n = n \cdot \Delta x \rightarrow (L/N)[0, \dots, N-1] \tag{III.29}$$

Frequency discretization

$$k_m = 2\pi \cdot p_m = 2\pi \cdot m \cdot \Delta p \rightarrow \left(\frac{2\pi}{L}\right)\left[0, \dots, \left(\frac{N}{2}\right) - 1, -\left(\frac{N}{2}\right), \dots, -1\right] \tag{III.30}$$

For n, m we have $(n, m = 0,1, \dots, N-1)$.

In the next and final step we present the main algorithm for the spectral method that is given by:

$$\frac{\partial \tilde{u}}{\partial z} = i e^{ik_m^2 z} FFT\left\{\left[V(n\Delta x) + \left|IFFT\left[\tilde{u}\, e^{-ik_m^2 z}\right]\right|^2\right] IFFT\left[\tilde{u}\, e^{-ik_m^2 z}\right]\right\} \tag{III.31}$$

$$\psi(n\Delta x, z) = IFFT\left[\tilde{u}(p_m, z) e^{-ik_m^2 z}\right] \tag{III.32}$$

The equation (III.31) is a nonlinear Ordinary Differential Equation and is typically solved by implementing a numerical method, in this case we have used the 4th order of Runge-Kutta method. The analysis we have described above is perfectly matched with our case-Schrödinger like equation, paraxial equation of diffraction, equation(III.4). We have presented and analyzed the Nonlinear Schrödinger equation(NLSE) as the general case, in which our equation of interest as presented in Chapter III is derived as a special case, without considering the nonlinear term and of course, ψ represents the electric field amplitude, $V(x)$ is the complex periodic optical potential with period D, $V(x) = V(x + D)$. This complex potential is a $\mathcal{PT}$ symmetric potential given the fact that its real part or refractive index profile is an even function of x and the loss/gain profile is antisymmetric, that means $V(x) = V^*(-x)$.

IV.Angular Sensitivity of Diffraction Patterns and EPs

i.Angular Sensitivity

Peculiar new phenomena, such as nonreciprocity, power oscillations and phase dislocations are revealed during dynamic beam evolution. In this paragraph we are investigating the spatial evolution of a wide incident beam, given the specific periodic $\mathcal{PT}$ potential $V(x) = 4[cos^2 x + iV_o \sin(2x)]$. As we demonstrate in this work, when we consider a wide(includes several channels) Gaussian beam at an arbitrary angle of incidence, we notice asymmetric diffraction patterns, for example double refraction and secondary emission. This is a direct result of the asymmetry of the associated FB modes and the physical non-reciprocity of the lattice. The aim of this section is to examine how the intensity distributions alters, when we select a different angle of incidence. In other words, we investigate in which angles our physical system is high and low sensitive under wide beam excitation. For this reason we have defined appropriately the sensitivity as we describe below.

The first step is to examine what happens under wide beam excitation to a Hermitian lattice and then compare it with the Non-Hermitian case of a $\mathcal{PT}$ symmetric lattice. In order to verify our results for these angles we imposed the stationary projection coefficients that have been numerically evaluated for the first three bands(where most of the energy of the beam is distributed), these results are shown in the next chapter.

To begin with we first consider, a wide incident beam which is a Gaussian-like beam. The electric field of the beam(which obeys the paraxial equation of diffraction) is defined by: $u(k_x, x, z) = \upsilon_o \cdot e^{-(x/w)^2} \cdot e^{ik_x \cdot x}$ equation (IV.1), z is the propagation distance, x stands for the spatial coordinate and w , which is the beam width.

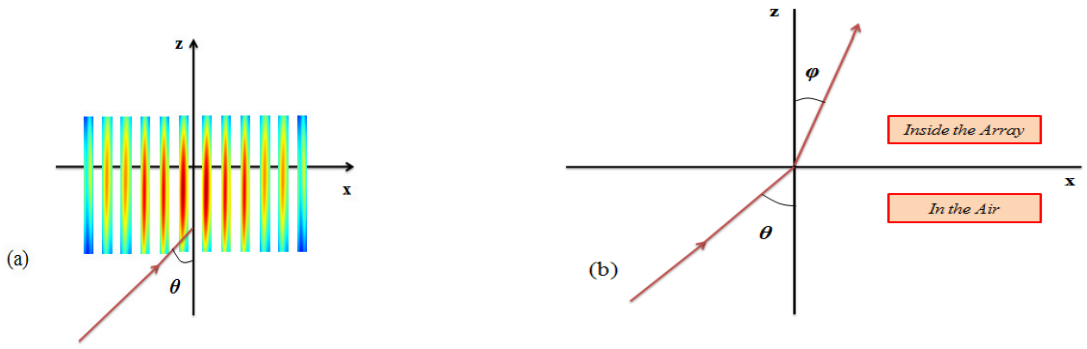

Fig6(a),(b):(a)Side-coupling geometry, angle θ describes the actual angle of incidence of the excitation beam in the air.(b)Hence angle φ is the specific angle we introduce to the BPM method, it expresses the angle inside the array. k_x is related to φ , as we can see in detail below(equation IV.3).

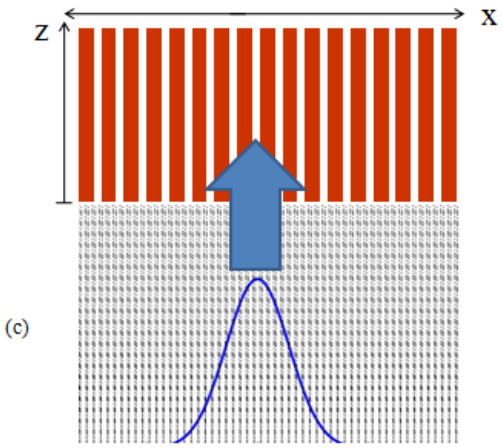

Fig6(c): Excitation condition, adjusting the input beam in order to match the modal shape of the desired FB modes.

By simply taking the components of $\boldsymbol{k}$(Bloch wave-vector) in x and z axes, we get that, $k_x = ksin\varphi$ and $k_z = kcos\varphi$, where φ is the angle between the two vectors. Also, k=$k_o n_o$ and k_o=2π/λ_o, with λ_o being the light wavelength and n_o is the background refractive index(see also normalizations in Chapter III, section Wave propagation in linear $\mathcal{PT}$ symmetric-periodic Media).

We deduct that $e^{i\boldsymbol{k}\cdot\boldsymbol{r}}$=$e^{i(k_x \cdot x + k_z \cdot z)}$ (IV.2). In the next step we are expressing the conditions for the physical tilting and the phase tilting we are introducing in the BPM method. From the above we can get that (with the condition that we are only dealing with the paraxial approximation where z=0):

For the physical tilting ,

$e^{ik_x \cdot x} = e^{i\, ksin\varphi \cdot x} = e^{i\cdot\left(\left(\frac{2\pi}{\lambda_o}\right)\cdot n_o \cdot sin\varphi\right)\cdot x}$, while for the tilting regarding the BPM method we get that:

$e^{ik_x\cdot\eta}$= $e^{ib\cdot\left(\frac{x}{x_o}\right)} = e^{i\cdot\left(\frac{k_x}{x_o}\right)\cdot x}$, where $\eta = \frac{x}{x_o}$ as presented in Chapter III .

When these conditions meet we get: $e^{i\cdot\left(\left(\frac{2\pi}{\lambda_o}\right)\cdot n_o \cdot sin\varphi\right)\cdot x} = e^{i\cdot\left(\frac{k_x}{x_o}\right)\cdot x} \Longrightarrow$

$\Longrightarrow \frac{2\pi}{\lambda_o} \cdot n_o \cdot sin\varphi = \frac{b}{x_o}$, if $x_o = \frac{D}{\pi}$ (see normalized paraxial equation III.3), then

we deduct the following relation for the parameter $\varphi = sin^{-1}\left(\frac{\lambda_o \cdot \frac{k_x}{k_o}}{2\, n_o \cdot D}\right)$ (IV.3), where we have used $(k_x\, /k_o)$ in order to get the result in the appropriate units, in rads.

The angle φ, describes the specific angles or the phase, we are investigating the sensitivity. It is the beam tilt we insert to the BPM method as described and investigated numerically, it concerns the angle inside the array as illustrated in Figure 6(a). On the other hand, in order to find the angle of incidence of the beam in the air(parameter θ) and not in the array, we have to apply Snell's law, Fig.6(b). Given that, the background refractive index equals n_o =3.28, from Snell's law we deduce that: $\theta = sin^{-1}(3.28\ sin\varphi)$ (IV.4), in rads. Hence, we are more familiar with degrees, so we have converted the rads to degrees, given that $1\ rad = \frac{180^\circ}{\pi}$. Considering the specific periodic $\mathcal{PT}$ potential, $V(x) = 4[cos^2x + iV_o \sin(2x)]$ we have mentioned above and for V_o =0.0 since we are first examining a Hermitian lattice. The Hermitian case of the wide beam excitation in a Hermitian lattice is first described(Figs7(b),(c),(d),(e),(f)). We notice a symmetric diffraction pattern when the angle of incidence is φ =0.0° and $\varphi = \pm 0.67°$ as illustrated in Figs7(b),(c),(d). We should note that, the diffraction patterns become asymmetric for $\varphi = \pm 0.34°$, Figs(e),(f).

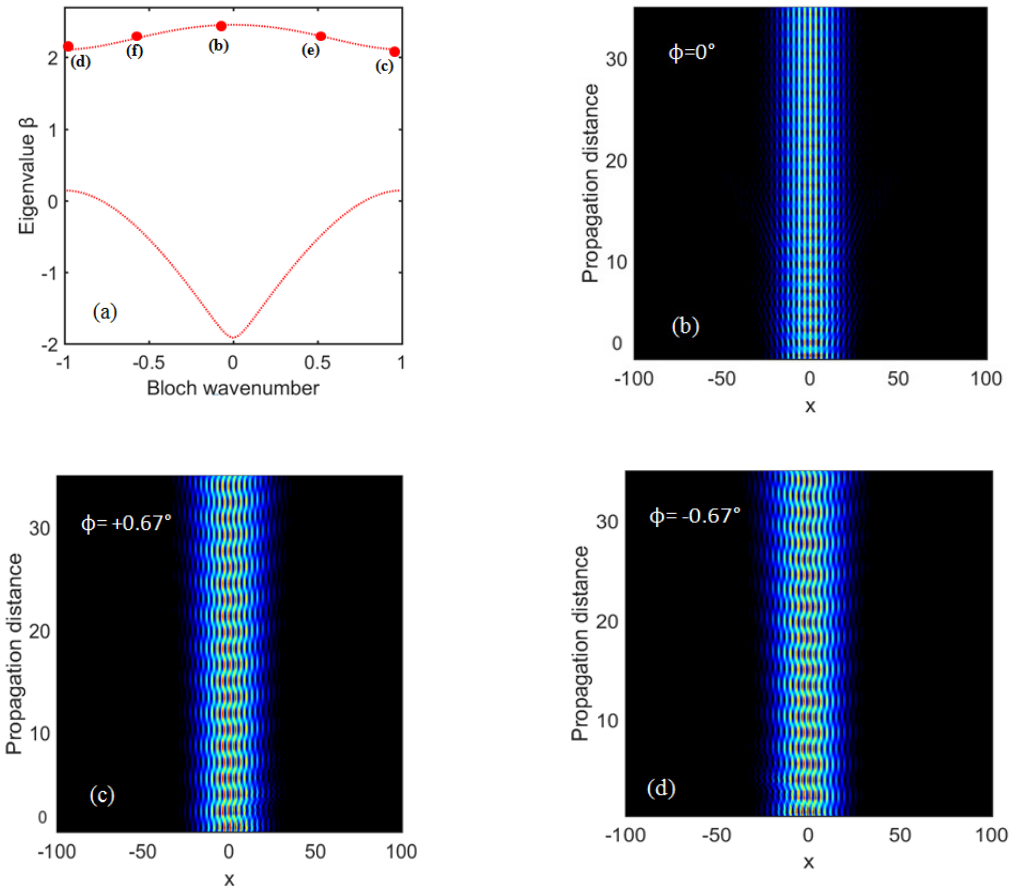

Figs7(a),(b),(c),(d):(a)Band structure of a Hermitian lattice, for the given potential. With red dot are depicted the Bloch's wavenumbers that correspond to the following cases. (b)Diffraction pattern in a Hermitian lattice under wide beam excitation when the angle of incidence is φ =0.0°.(c),(d) φ=±0.67° . In all three cases we get symmetric diffraction patterns.

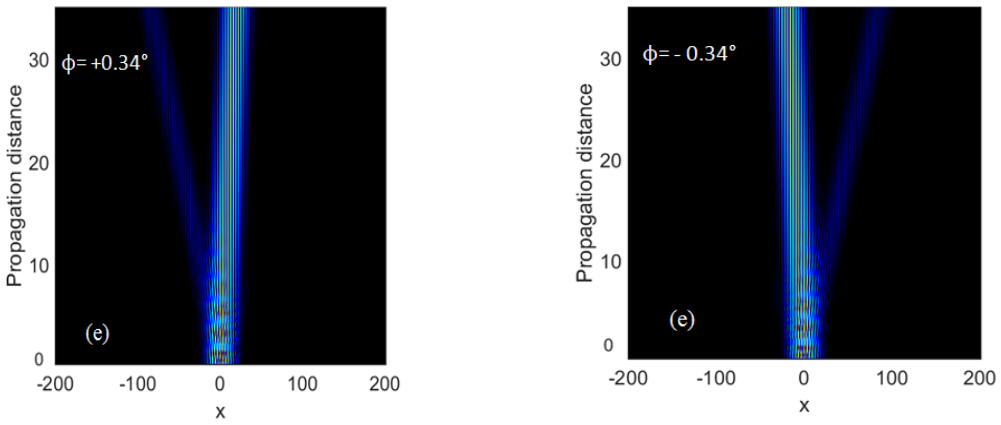

Figs7(e),(f): Asymmetric diffraction patterns for φ=±0.34° respectively.

On the other hand, in the Non-Hermitian case of a $\mathcal{PT}$ symmetric lattice the intensity distributions under wide beam excitation are presented below. We demonstrate as shown in Figures 8(b),(c),(d),(e)(f) that for a different angle of incidence, when of course V_o =0.495 , we get a completely different intensity distribution compared to the Hermitian case.

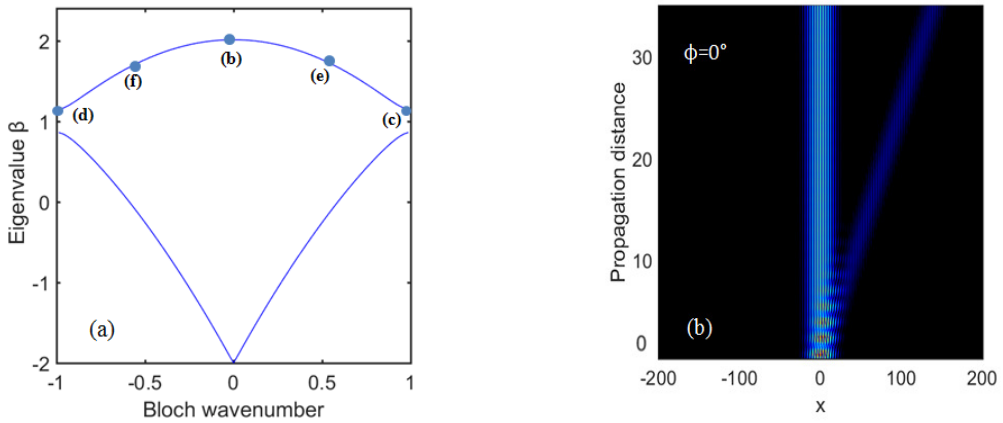

Figs8(a),(b): (a) Band structure of a Non-Hermitian lattice considering the specific periodic $\mathcal{PT}$ potential highlighted above.(b) Intensity distribution for φ=0.0°.

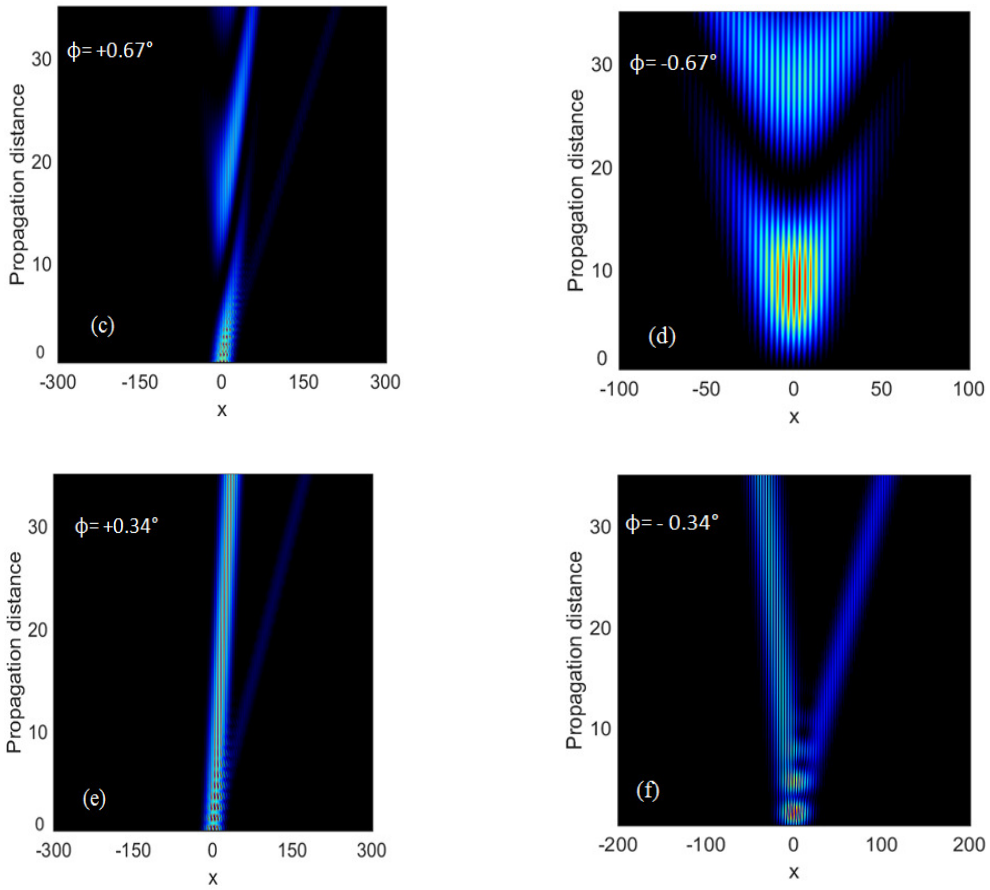

Figs8(c),(d),(e),(f): Strange diffraction patterns in a $\mathcal{PT}$ symmetric lattice under wide beam excitation, for $V_o = 0.495$. In the Non-Hermitian case asymmetric diffraction patterns due to double refraction and secondary emission are expected. (c),(d)When $\varphi = \pm 0.67°$ in the first case the diffraction pattern is highly asymmetric, while in the other is symmetric around axis x=0 .(e),(f) Intensity evolution patterns for $\varphi = \pm 0.34°$ respectively, in both cases the beam is splitting in two components, hence producing two different diffraction patterns.

In the next step, we demonstrate that around specific angles our physical system is high and low sensitive under wide beam excitation in the Non-Hermitian case for $V_o = 0.495$. This means that in these angles the intensity distribution alters more drastically and as shown in the next chapter with the computation of the energy distribution. We have scanned a wide region of angles where our system could be more sensitive. The electric field as demonstrated above is a function of the angle φ inside the array, z which is the propagation distance, x stands for the spatial coordinate . For this reason the sensitivity can be defined as the overlap integral of the electric field of the beam under wide beam excitation where we keep all the parameters fixed and we only change the angle φ, with a step of ε=0.057° each time. In equation (IV.5) the normalized form of the overlap integral is presented.

$$Sensitivity \equiv S(\varphi, x, z) = \frac{\int_{-\infty}^{+\infty} |u(\varphi, x, z) \cdot u(\varphi + \varepsilon, x, z)|\, dx}{\int_{-\infty}^{+\infty} |u(\varphi, x, z)|^2\, dx}$$

marked as equation (IV.5). Another way of describing the sensitivity is by considering the normalized form of the absolute difference of the integrals of the electric field. In this form it is described by equation (IV.6).

$$S(\varphi, x, z) = \frac{\int_{-\infty}^{+\infty} |u(\varphi, x, z)|^2\, dx - \int_{-\infty}^{+\infty} |u(\varphi + \varepsilon, x, z)|^2\, dx}{\int_{-\infty}^{+\infty} |u(\varphi, x, z)|^2\, dx}$$

denoted as equation (IV.6).

At first we present some indicative diffraction patterns(Fig.9,10) in the Hermitian and the non-Hermitian regime. Our aim is to show how drastically the intensity distribution changes with respect to the angle φ. In certain cases our system appears more sensitive than others. These results are analyzed in the Sensitivity-Bloch wavenumber diagrams that follow.

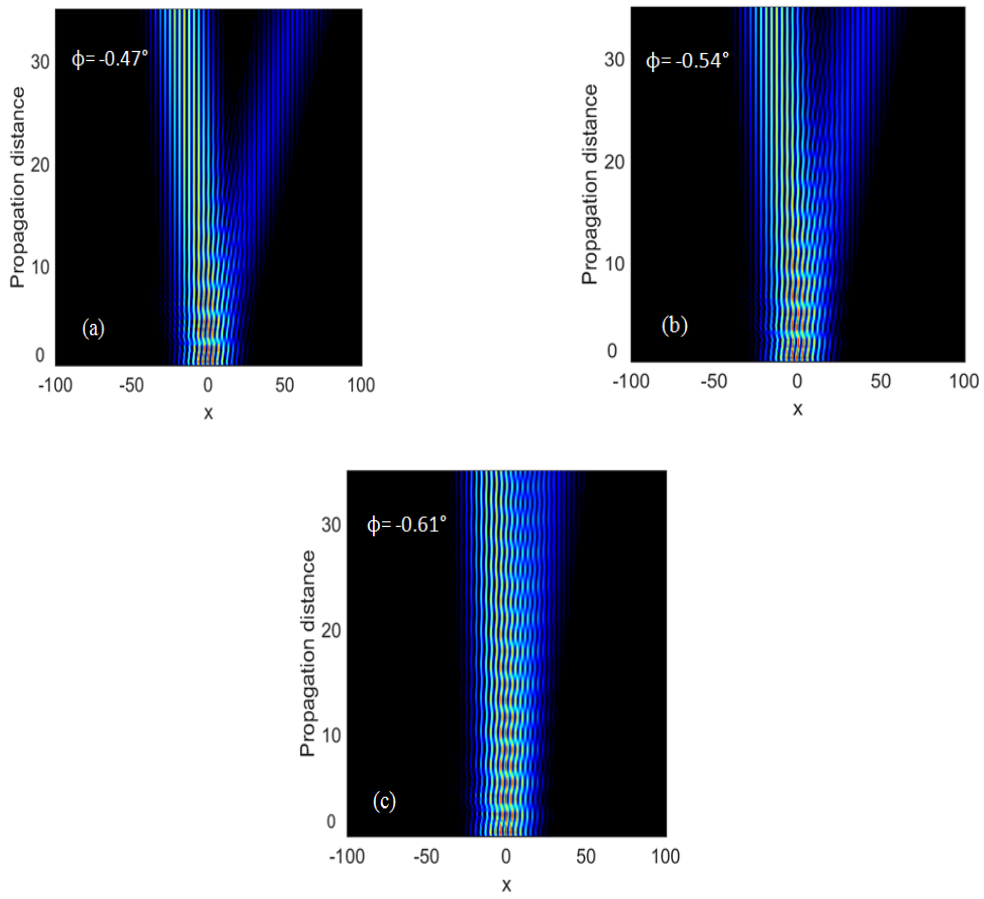

Figs9(a),(b), (c): Diffraction patterns in the Hermitian lattice, when the angle of incidence in the array is (a) φ= -0.47° and (b) φ=-0.54°. In both cases the beam has two distinctive regions, a central region and a tilted to the right. (c)Diffraction pattern when the angle of incidence in the array is φ=-0.61°. Now the pattern is to be shaped in to a central region only as it approaches the angle φ=-0.67°.

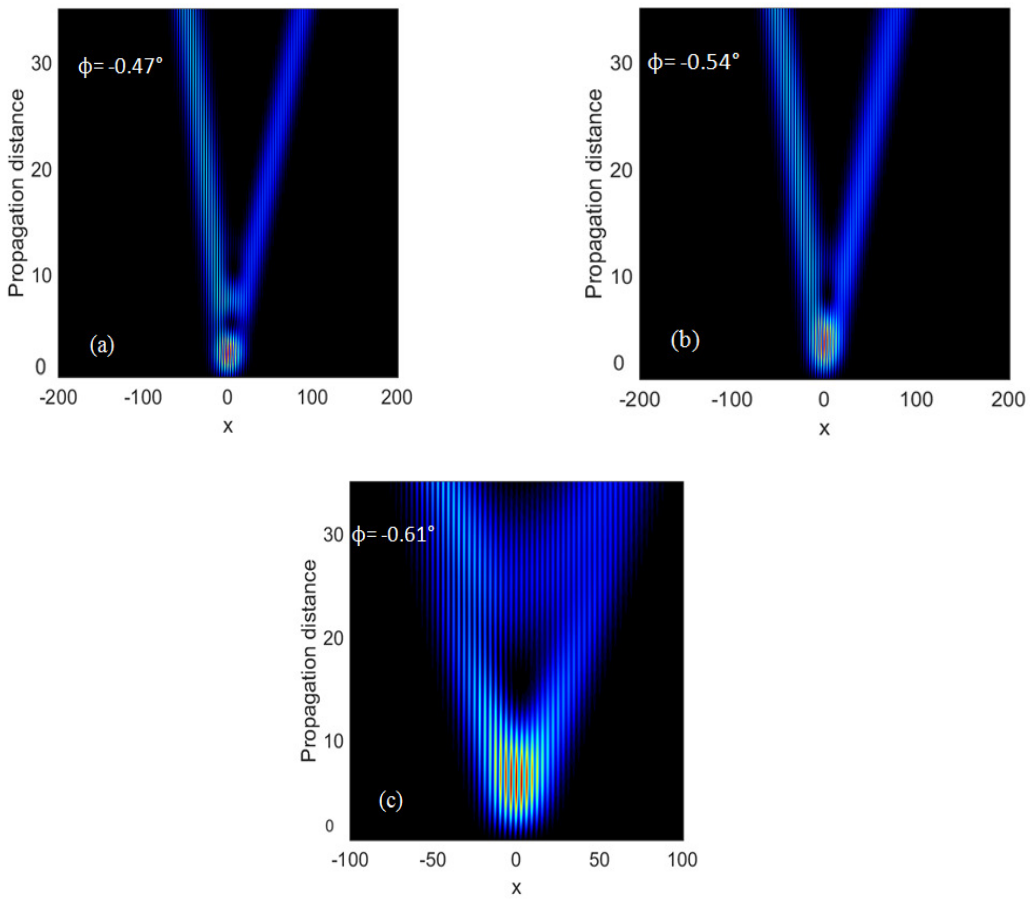

Figs.10(a),(b),(c): Rapidly evolving diffraction patterns in the non-Hermitian lattice from (a) φ=-0.47° where the beam is splitting in two components to (b) φ=-0.54° where a main lobe is also appears, to finally (c)where φ=-0.61° where the beam has now a shaped lobe in the centre and two symmetric regions. The diffraction pattern is highly symmetric around axis x=0, for φ=-0.67°.

We continue by presenting, the sensitivity-phase diagram where the high and low sensitivity values of the parameter φ and subsequently values of φ are depicted. Once again, at first the Hermitian case is described where we should note that it appears extremely low values of sensitivity(the Sensitivity is presented as the normalized form of the overlap integral-Figs11(a)). In order to plot Figures 11 we have taken into consideration how we have defined the Sensitivity(equations IV.5 and IV.6). In Figs11(b),(c) is depicted the normalized form of Sensitivity as a function of Bloch wavenumber. Hence in Fig11(b) the Sensitivity is expressed as the normalized form of the difference of the absolute values while in Fig11(c) it is expressed as the normalized form of the overlap integral.

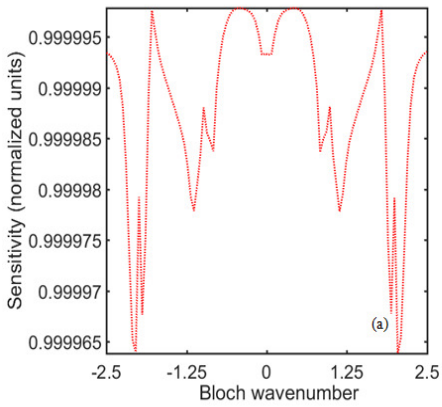

Figs11(a): Sensitivity is presented as function of phase in the Hermitian case, indicating extremely low values(to the sixth digit) of Sensitivity(as defined here, normalized form of the overlap integral).

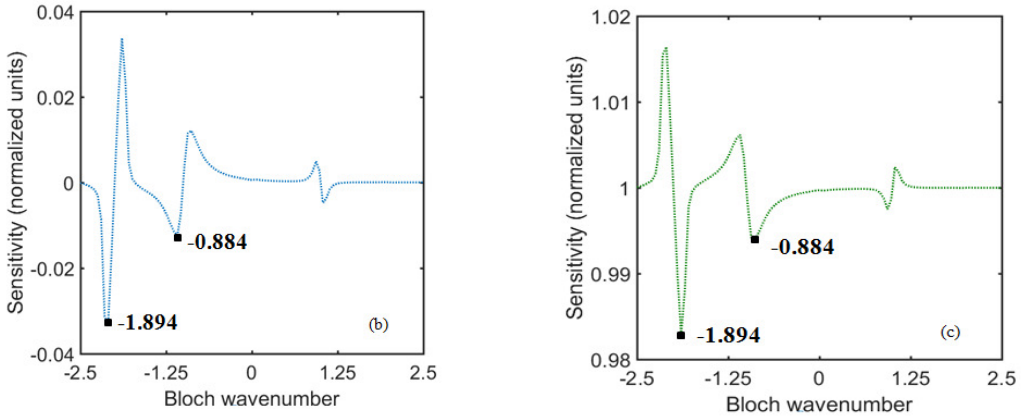

Figs11(b),(c): Sensitivity as a function of phase expressed in two different normalized forms.(b) Sensitivity is presented as the normalized form of the difference of the absolute values , while in (c) it is depicted as the normalized form of the overlap integral. In both cases the two values of maximum sensitivity are highlighted and are in perfect match.

For these two values of phase that resulted we should first investigate theirs dynamic beam evolution, starting from the corresponding diffraction patterns. The analysis continues in the next section along with the implementation of the stationary projections coefficients for the values of phase examined in this section. With this method we can numerically evaluate in which bands, typically the first three, the energy is distributed.

ii.Biorthogonal Projections

In this section, we have numerically computed the beam's energy content for different bands. Given the analysis preceded in Chapter III, Orthonormality and Projection in a Finite $\mathcal{PT}$ Lattice, we have applied the stationary projection coefficients $|A_n(k)|^2$ as described in equation III.14 for a finite $\mathcal{PT}$ lattice, for the numerical computation for the first three bands(where most of the energy of the beam is distributed). In Figs.12(a),(b),(c)(d) are presented the input fields for the values of phase as examined in the last section, and the corresponding projection coefficients distributions.

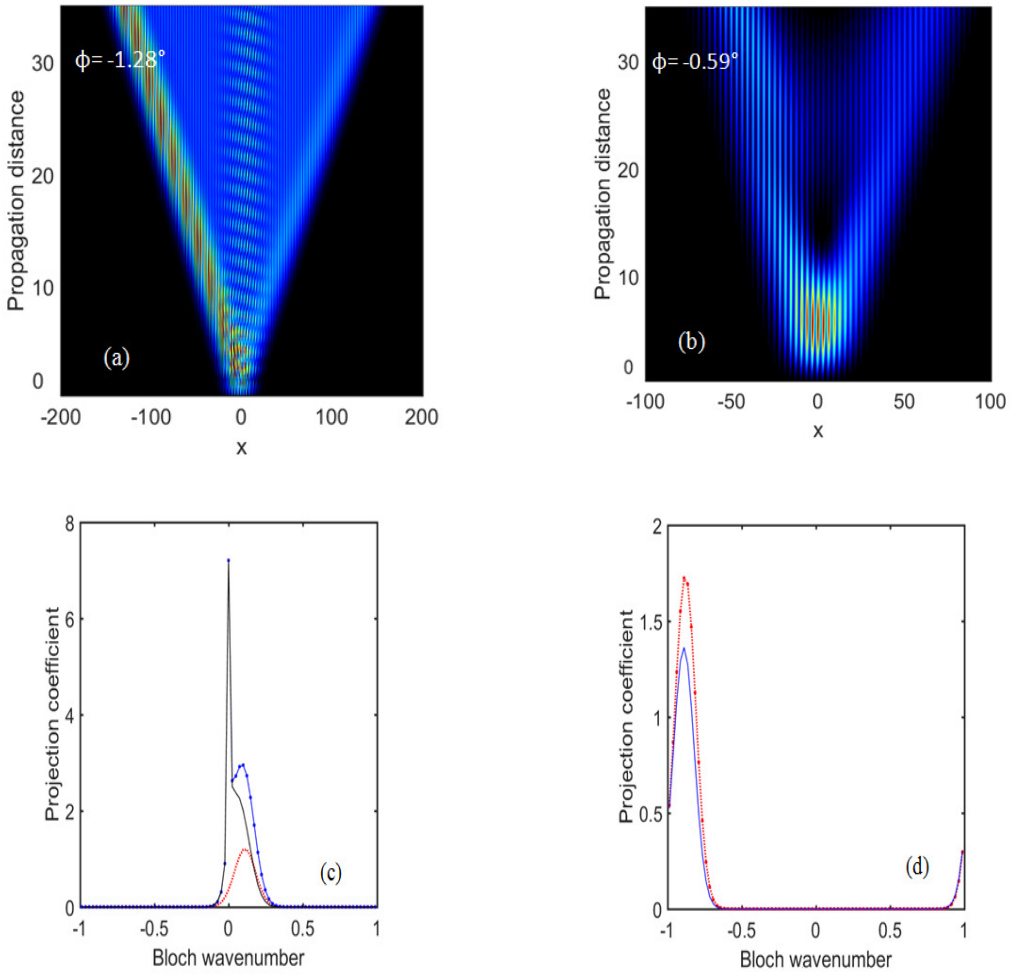

Fig.12(a),(b),(c),(d): Intensity evolution of two different input beams, which results to (a) a diffraction pattern that has a main region with high input profile including distinctive regions, (b) a diffraction pattern that has two different parts which unite and become symmetric around x=0 axis. (c),(d) corresponding projection coefficients diagrams for these input beams are illustrated, the first band (red solid line), second band(blue dotted line), third band(black dotted line).

In Figs12(a),(b) we get to see the intensity distributions for the two difference angles of incidence, given the specific periodic potential and when of course V_o =0.495 . For the first one (a) the diffraction pattern has a main region with high input profile including distinctive regions, hence asymmetric. The corresponding projections coefficients for the first three bands are asymmetric. Most of the energy is distributed in the third band, while the second band appears to have a great contribution as well. Given that, we can explain the intense profile in the left of the main profile of the input beam. On the other hand for the case (b) the profile of the input beam has two different parts which unite and become symmetric around x=0 axis. From the projection analysis we get that for the distribution for the first two bands can be divided in two regions where in the edges of the Brillouin zone is asymmetric, while in the centre of the Brillouin zone for k=0 is symmetric. We should take into account that the first band has higher contribution at first and then the contribution of the two bands is equally contributed. This behavior explains the input beam profile.

In the next section we are examining the behavior of power with respect to the propagation distance z. We have investigated these two different examples of power oscillations in a $\mathcal{PT}$-periodic potential of the form $V(x) = 4[cos^2 x + iV_o \sin(2x)]$ and for V_o =0.495.

iii.Power Oscillations

The power P is not a conserved quantity in a PT symmetric optical lattice, even in the case of real spectrum (unbroken symmetry). In this paragraph we aim to study the variation of power as a function of the propagation distance z. As described in Chapter III, this can be analytically derived by computing the integrated power while taking into account the usual condition for the inner product: $\langle f,g\rangle=\int_{-\infty}^{+\infty} f(x)^* g(x)dx$, equation (III.16) - Chapter III. It is important to note that we should also consider the non-orthogonality of the corresponding FB modes. In the next step we calculate the power of an arbitrary input beam, considering it as a linear superposition of non-orthogonal FB mode. For the total power P, we have deducted the following:

$$P=\frac{2\pi}{D}\sum_{n=1}^{+\infty}\int_{-\pi/D}^{\pi/D}|A_n(k)|^2\left(\int_{-D/2}^{+D/2}|\Phi_{kn}(x)|^2dx\right)dk$$

$$+\frac{2\pi}{D}\sum_{\substack{n=1\\n\neq m}}^{+\infty}\sum_{m=1}^{+\infty}\int_{-\pi/D}^{\pi/D}A_n A_m^*\left(\int_{-D/2}^{+D/2}\Phi_{k,m}^*\Phi_{k,n}(x)dx\right)e^{i\Delta\beta_{n,m}(k)z}\,dk \qquad \text{(IV.7)}$$

where $\Delta\beta_{n,m}=\beta_n(k)-\beta_m(k)$. The first term corresponds to the usual power-spectral summation that exists in a real lattice. Considering the conditions for the usual inner product and orthogonality in a real lattice, the second term of (IV.7) becomes zero. Also $\int_{-D/2}^{+D/2}|\Phi_{kn}(x)|^2dx=1$. Therefore the relation (IV.7) only has terms corresponding to the Parseval's identity in a real lattice as defined in Chapter V. As highlighted above, the FB modes in a $\mathcal{PT}$ lattice are non-orthogonal. In equation (IV.7) the second term is consistent with this behavior. We have to note that because of this term the power P has oscillations in the z coordinate. However, power oscillations are not periodic in general.

As mentioned above we present the power oscillations of the first and second beam we are examining with respect to the analysis preceded. From Figs12(e),(f) we get to see that in the first case the input beam profile leads to weak power oscillations, while the other appears to have a greater amplitude of power oscillations.

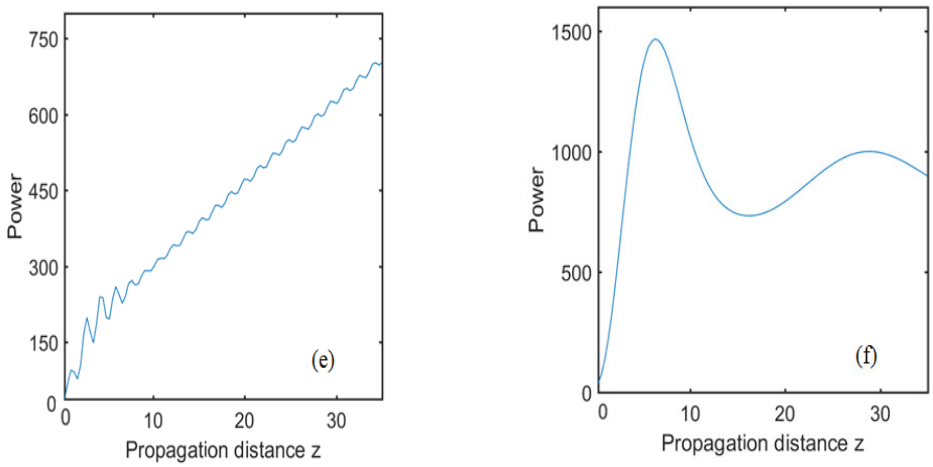

Figs12(e),(f): Integrated power oscillations as a function of the propagation distance, for the input beam profiles cases (a) and (b) respectively.

V.Conclusion and outlook

We have investigated the angular sensitivity of the diffraction pattern in a PT symmetric optical lattice under wide beam excitation near the exceptional point. We give emphasis on the characteristics of the waveguide arrays where the entire structure obeys the parity-time symmetry, angular sensitivity offers a fruitful ground for potential applications, such as ultrasensitive sensors. I also hope that my thesis will have a contribution to a better understanding of wave diffraction in excitation of higher bands(such as the third and fourth band as well).

References

[1] K.G.Makris, R.El-Ganainy , D.N.Christodoulides, PT symmetric optical lattices. *Physical Review Letters* A 81, 063807 (2010).

[2] K.G.Makris, R.El-Ganainy, D.N.Christodoulides, Beam dynamics in PT Symmetric Optical Lattices. *Physical Review Letters* 100, 103904 (2008).

[3] V.V.Konotop, J. Yang, D.A.Zezyulin, Non linear waves in PT symmetric systems. *Reviews of Modern Physics*, 88, July-September (2016).

[4] R.El-Ganainy, K.G.Makris, D.N.Christodoulides, Theory of coupled optical PT-symmetric structure. *Optics Letters* 32, 2632 (2007).

[5] Z.H.Musslimani, K.G.Makris, R.El-Ganainy, D.N.Christodoulides, Optical Solitons in PT Periodic Potentials. *Physical Review Letters* 100, 03402 (2008).

[6] A.Guo *et al.* , Observation of PT Symmetry Breaking in Complex Optical Potentials. *Physical Review Letters*, 103,093902 (2009).

[7] C.E.Rütter *et al.* , Observation of parity-time symmetry in optics. *Nature Physics* 6, 192-195 (2010).

[8] S.Klaiman, U.Günther, N.Moiseyev, Visualization of Branch Points in PT-Symmetric Waveguides. *Physical Review Letters* 101, 080402 (2008).

[9] Z.Lin *et al.*, Unidirectional Invisibility Induced by PT-Symmetric Periodic Structures. *Physical Review Letters* 106, 213901 (2011).

[10] A.Regensburger *et al.*, Parity-time synthetic photonic structures. *Nature Physics* 488, 167-171 (2012).

[11] S.Longhi, PT-symmetric laser absorber. *Physical Review Letters* A 82, 031801 (2010).

[12] W.Wan *et al.* , Time-Reversed Lasing and Interferometric Control of Absorption. *Science* 331, 889-892 (2011).

[13] H.Ramezani, T.Kottos, R.El-Ganainy, D.N.Christodoulides, Unidirectional nonlinear PT-symmetric optical structures. *Physical Review Letters* A 82, 043803 (2010).

[14] H.Hodaei, M.-A. Miri, M.Heindrich, D.N.Christodoulides, Parity-time-symmetric microring lasers. *Science* 346, 975-978 (2014).

[15] L.Feng, Z.J.Wong, R.-M.Ma, Y.Wang, X.Zhang, Single-mode laser by parity-time symmetry breaking. *Science* 346, 972-975 (2014).

[16] C.M.Bender, D.C.Brody, H.F.Jones, Complex Extension of Quantum mechanics. *Physical Review Letters* 89, 270401 (2002).

[17] C.E.Rütter, K.G.Makris, R.El-Ganainy, D.N.Christodoulides, M.Segev, D.Kip, Observation of parity–time symmetry in optics. *Nature Physics* 6, 192-195 (2010).

[18] D.N.Christodoulides, F.Lederer, Y.Silberberg, Discretizing light behavior in linear and nonlinear waveguide lattices. *Nature(London)* 424, 817-823 (2003).

[19] A.Yariv, Optical Electronics in Modern Communications(Oxford University Press, Oxford, 1997); P.Yeh, Introduction to Photorefractive Nonlinear Optics, Wiley Series in Pure and Applied Optics (Wiley, New York,2001).

[20] Berry, M.V: Physics of non Hermitian degeneracies. *Czechoslovak Journal of Physics* 54, 1039-1047 (2004).

[21] Berry, M.V: Optical lattices with PT symmetry are not transparent. *Journal of Physics* A*: Mathematical and Theoretical* 41, 244007 (2008).

[22] Kohn, W. : Analytic properties of Bloch waves and Wanier functions. *Physical Review Letters* 115, 809-821 (1959).

[23] Kotani, S.: Generalized Floquet theory for stationary Schrödinger operators in one dimension. *Chaos Solitons Fractals* 8, 1817-1854 (1997).

[24] Cottey,A.A.: *Floquet's theorem and band theory in one dimension. American Journal of Physics* 39, 1235-1244 (1971).

[25] Eastam, M.: *The* Spectral Theory of Periodic Differential Equations. *Scottish Academic Press*, Edinburgh (1973).

[26] Meiman, N.N.: The theory of one dimensional Schrödinger operators with a periodic potential. *Journal of Mathematical Physics* 18, 834-848 (1977).

[27] Ahmed, Z.: Energy band structure due to a complex periodic, PT invariant potential. *Physical Review Letters* A 286, 231-235 (2001).

[28] Boyd, J.K.: One-dimensional crystal with a complex potential. Journal of Mathematical *Physics* 42, 15-19 (2001).

[29] Cervero, J.M.: PT symmetry in one-dimensional quantum periodic potentials. *Physical Review Letters* A, 317, 26-31 (2003).

[30] Khare,A., Sukhatame,U.: Analytically solvable PT-invariant periodic potentials. *Physical Review Letters* A 324, 406-414 (2004).

[31] Khare,A., Sukhatame,U.: Periodic Potentials and PT symmetry. *Journal of Physics* A*: Mathematical and General* 3910133-10142 (2006).

[32] Bender, C.M.: Introduction to PT symmetric quantum theory. *Contemporary Physics* 46, 277-292(2005).

[33] Bender, C.M.: Four easy pieces. *Journal of Physics A: Mathematical and General* 39,9993-10012 (2006).

[34] Bender, C.M.: Making sense of non Hermitian Hamiltonians. *Reports on Progress in Physics* 70, 947-1018 (2007).

[35] Bender, C.M., Boettcher, S.: Real spectra in non-Hermitian Hamiltonians having PT symmetry. *Physical Review Letters* 80, 5243-5246 (1998).